# Superconductivity with Wannier-Stark flat bands

Si Min Chan,[1,2] Alexei Andreanov,[3,4] Sergej Flach,[3,4] and G. George Batrouni[1,2,5]
[1]*Centre for Quantum Technologies, National University of Singapore, 3 Science Drive 2, 117543 Singapore*
[2]*Department of Physics, National University of Singapore, 2 Science Drive 3, 117551 Singapore*
[3]*Center for Theoretical Physics of Complex Systems, Institute for Basic Science (IBS), Daejeon 34126, Korea*
[4]*Basic Science Program, Korea University of Science and Technology (UST), Daejeon 34113, Republic of Korea*
[5]*Université Côte d'Azur, CNRS, Institut de Physique de Nice (INPHYNI), 06103 Nice, France*

(Received 7 August 2023; revised 7 February 2024; accepted 8 February 2024; published 23 February 2024)

We investigate superconducting transport in the DC field induced Wannier-Stark flat bands in the presence of interactions. Flat bands offer the possibility of unconventional high temperature superconductivity, where the superfluid weight, $D_s$, is enhanced by the density overlap of the localized states. However, construction of flat bands typically requires very precise tuning of Hamiltonian parameters. To overcome this difficulty, we propose a feasible alternative to realize flat bands by applying a DC field in a commensurate lattice direction. We systematically characterize the superconducting behavior on these flat bands by studying the effect of the DC field and attractive Hubbard interaction strengths on the wave function, correlation length, pairing order parameter, and the superfluid weight $D_s$. Our main result is that the superfluid weight is dramatically enhanced at an optimal value of the interaction strength and weak DC fields.

DOI: 10.1103/PhysRevB.109.075153

## I. INTRODUCTION

Flat band systems are systems that exhibit at least one band where the particle energy does not depend on its momentum; the flat band is, therefore, dispersionless. Topologically nontrivial flat bands have proved to be promising in the search for high temperature superconductivity [1–16]. The merit of superconductivity on isolated flat bands is twofold: (a) due to quenched kinetic energy any finite interaction is relevant, resulting in a strongly correlated system, where superconducting transport arises from the correlated hopping of the fermions; and (b) both the critical temperature ($T_c$) and superfluid weight ($D_s$) depend *linearly* on the attractive interaction ($U$), and are thus exponentially enhanced compared to dispersive bands with weak attraction between electrons [7–9,14,15,17]. In these systems, flat band superconductivity at weak interaction was shown to be dominated by a single isolated flat band [2,5–7]. The superconducting properties of the many-body system, in the presence of a weak attraction, are largely dependent on both the wave function and the band topology in the noninteracting limit [6–9,11].

In a very wide range of flat-band systems, the localized state is compact, i.e., the particle is localized on a small number of sites beyond which its wave function is exactly zero. For example, on the Creutz lattice, the localized state extends over only four sites on two neighboring unit cells [2,16]. On the sawtooth lattice, the compact localized state (CLS) is supported on only three sites [18,19] also on two neighboring unit cells. In systems with isolated flat bands with compact localized states, the CLS must span more than one unit cell in order for the linear dependences $D_s \propto U$ and $T_c \propto U$ to emerge [3,7,11,20]. In systems where the CLS is confined to only one unit cell, superconductivity is suppressed [3] and does not depend linearly on $U$. To optimize $D_s$ further, the system parameters must be chosen such that the overlap between neighboring CLS is maximized, resulting in the maximization of the density overlap of the Wannier functions [3,6].

Often, the construction of flat bands requires subtle fine tuning of Hamiltonian parameters. To design flat bands, a specific set of rules have to be followed, and hopping potentials are fixed with precise values chosen to ensure flatness of the band [21–25]. While these systems have been experimentally realized in superconducting wire networks, atomic lattices and optical lattices, flat bands with longer-range hopping, e.g., beyond nearest neighbors, which provide control over the CLS, become difficult to fabricate [26–32]. Flat band superconductivity was observed experimentally in twisted bilayer graphene, but the bilayers have to be stacked precisely at a "magic" angle at which band flatness is maximized (though not being perfectly flat) [1].

It is, therefore, interesting to examine the possibility of obtaining flat band systems without the need for fine tuning. In addition, as mentioned above, in a vast class of flat band systems, the localized state is compact, its wave function being supported, typically, on up to two unit cells, beyond which it is strictly vanishing. It is, therefore, also useful to examine flat band systems where the localized state is *not* compact; in other words where the localized state wave function decays gradually, thus increasing overlap among the localized states populating the system. Such increased overlap has been shown to enhance superconductivity [18,19].

A rather large class of systems and models exist where approximate flat bands are present without the need to fine tune parameters (although other constraints are present) [33–37]. In addition, the localized states in these systems are not compact and therefore favor superconductivity. However, these systems differ in two important ways from the systems we study here. First, the flat band is a surface band, while, in our system below, the flat band is in the bulk. Second, in these

 ©2024 American Physical Society

systems there is one isolated flat band. In the system we will examine below there are many closely separated flat bands and the gaps between them are easily adjusted, as is the wave function spread across several bands.

When a static DC field is oriented in a lattice commensurate direction of a $D \geqslant 2$ Bravais lattice, it was shown that flat bands of dimension $D-1$ are formed in the direction perpendicular to the DC field, and the emergence of flat bands is independent of the field strength [38]. These Wannier-Stark flat bands do not have CLS, only superexponentially localized wave functions which depend on the field strength. We propose that this method of generating flat bands comes with two advantages for superconductivity: (a) no fine tuning is required and (b) there is no CLS which, therefore, increases the density overlap of the wave functions and potentially enhances superconductivity. In practice, one can, for example, emulate this in ultracold atomic gas experiments, by tilting the system at an angle so that the gravitational field acts in the chosen commensurate direction of the optical lattice [39–42].

Previous studies have shown extensively that the multiband mean-field theory describes the superconducting properties of flat band systems remarkably well in comparison with density matrix renormalization group (DMRG) computations and determinant quantum Monte Carlo (DQMC) [2,3,5,6,9,12]. Thus, in this study, we investigate interacting fermions in the Wannier-Stark flat band systems using the full multiband mean-field theory [2,3]. In particular, we show the dependence of the superfluid weight, pairing order parameters, lattice filling, and correlation functions on both the DC field and interaction strengths.

Our main result is that the flat band enhancement of superconductivity persists in Wannier-Stark systems despite the trivial topology of the underlying lattice. Consequently, superconductivity can be readily improved in Bravais lattices by applying a static field in a commensurate direction, which induces Wannier-Stark flat bands. These flat bands act as superconducting transport channels with the additional advantage of a tuneable spread of the wave function and band gaps. At weak Hubbard attraction and sufficiently strong DC field, the pairing order parameter is enhanced, while the superfluid weight is large due to the transport being supported by multiple flat bands, growing linearly with the interaction. Moreover, for sufficiently large DC field strength, the correlation length is smaller than a lattice spacing, typical for flat bands, indicating that bound Cooper pairs are very small, essentially on a single site.

The paper is organized as follows. We introduce the Hubbard Hamiltonian on the Wannier-Stark lattice in two and three dimensions in Sec. II. Additionally, we briefly outline how to compute the superconducting quantities. Thereafter, in Sec. III, we characterize the superconducting properties of Wannier-Stark flat bands and develop an understanding of its dependence on the DC field and Hubbard interaction strengths. Finally, in Sec. IV we conclude with the main takeaways from this study and the future outlook.

## II. MODEL AND METHODS

We begin by considering the two-dimensional (2D) square lattice with a DC field $E\mathbf{e_z}$ in the plane of the lattice and oriented in a commensurate direction, and the on-site attractive Hubbard interaction term. The Hamiltonian can be expressed with the single particle and interaction components, as

$$H - \mu N = H_S + H_I, \tag{1}$$

where

$$\begin{aligned} H_S &= -t \sum_{x,y,\sigma} (c^\dagger_{x,y,\sigma} c_{x+1,y,\sigma} + c^\dagger_{x,y,\sigma} c_{x,y+1,\sigma} + \text{H.c.}) \\ &\quad + \sum_{x,y,\sigma} (E\,\mathbf{e_z}\cdot\mathbf{r} - \mu) c^\dagger_{x,y,\sigma} c_{x,y,\sigma}, \\ H_I &= -U \sum_{x,y} c^\dagger_{x,y,\uparrow} c_{x,y,\uparrow} c^\dagger_{x,y,\downarrow} c_{x,y,\downarrow}. \end{aligned} \tag{2}$$

Here, $\mathbf{r} = xa\mathbf{e_x} + ya\mathbf{e_y}$, with $x, y \in \mathbb{Z}$ and $a$ is the lattice constant. $c^\dagger_{x,y,\sigma}$ ($c_{x,y,\sigma}$) creates (annihilates) fermions of spin $\sigma \in (\uparrow, \downarrow)$ on site $(x, y)$. $t$ is the hopping parameter, $\mu$ is the chemical potential which controls the filling of the lattice, and $U > 0$ is the Hubbard interaction strength. Note that the field $E$ couples to the local particle density and has the form of a local chemical potential. It can, therefore, be introduced into the system as an electric field, or as a local chemical potential for example by adding a linear term to the confining potential in a system of ultracold atoms loaded in an optical lattice. We define the orthogonal vectors $\mathbf{e_z}$ and $\mathbf{e_w}$ which are respectively parallel and perpendicular to the DC field direction. For the commensurate DC field direction, $\mathbf{e_w}$ is parallel to some lattice vector. For specific calculations, we set $\mathbf{e_z} = (\mathbf{e_x} - \mathbf{e_y})/\sqrt{2}$ and $\mathbf{e_w} = (\mathbf{e_x} + \mathbf{e_y})/\sqrt{2}$ in this study, where lattice sites can then be labeled with $z, w \in \mathbb{Z}$.

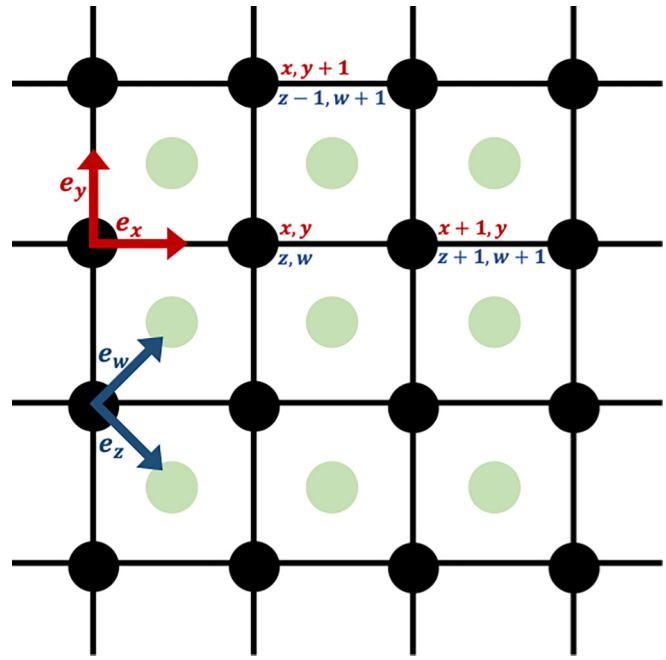


FIG. 1. Square lattice with DC field direction $\mathbf{e_z}$ indicated. Original and new coordinates of the square lattice are shown as $x, y$ and $z, w$. In the $z, w$ basis (which is in the same plane as the $(x, y)$ basis), both coordinates have to be simultaneously changed ($\pm 1$) to describe hopping in the original basis.

The Hamiltonian in the $z$, $w$ basis is

$$H_S = -\frac{t}{2}\sum_{z,w,\sigma}(c^\dagger_{z,w,\sigma}c_{z+1,w+1,\sigma} + c^\dagger_{z,w,\sigma}c_{z-1,w+1,\sigma} + \text{H.c.}) + \frac{1}{2}\sum_{z,w,\sigma}(Fz-\mu)c^\dagger_{z,w,\sigma}c_{z,w,\sigma},$$
$$H_I = -\frac{U}{2}\sum_{z,w} c^\dagger_{z,w,\uparrow}c_{z,w,\uparrow}c^\dagger_{z,w,\downarrow}c_{z,w,\downarrow} \tag{3}$$

with $F = \frac{aE}{\sqrt{2}}$.

In the $z$, $w$ basis, we apply the mean-field decoupling on the Hubbard interaction term (Appendix A), recognizing that the mean-field parameters $\Delta^z/U = \langle c_{z,w,\uparrow}c_{z,w,\downarrow}\rangle$ and $\rho^z_\sigma = \langle c^\dagger_{z,w,\sigma}c_{z,w,\sigma}\rangle$ should depend on $z$,

$$\widetilde{H}_I = -\frac{1}{2}\sum_{z,w}(\Delta^z c^\dagger_{z,w,\downarrow}c^\dagger_{z,w,\uparrow} + \Delta^{z*}c_{z,w,\uparrow}c_{z,w,\downarrow}) - \frac{U}{2}\sum_{z,w}(\rho^z_\uparrow c^\dagger_{z,w,\downarrow}c_{z,w,\downarrow} + \rho^z_\downarrow c^\dagger_{z,w,\uparrow}c_{z,w,\uparrow})$$
$$+ \frac{1}{2}L_w\sum_z(U\rho^z_\uparrow\rho^z_\downarrow + |\Delta^z|^2/U), \tag{4}$$

where $\widetilde{H}_I$ is the mean-field approximation of the interaction term, and $L_w$ is the number of sites in the $w$ direction. Here, $\Delta^z/U$ and $\rho^z_\sigma$ are the pairing order parameter and filling on sites with equal values of $z$. $\Delta^z$ itself is an energy and represents the spin gap, i.e., the energy needed to break the pair. The factor $\frac{1}{2}$ in Eqs. (3) and (4) accounts for double counting and arises when we sum over $z$ and $w$ due to the two sublattices, as shown in Fig. 1. While the translational symmetry in the $\mathbf{e_z}$ direction is broken due to the DC field, the system remains translationally invariant in the $\mathbf{e_w}$ direction. Under Fourier transformation in $w$, we can express the Hamiltonian as

$$2(H-\mu N) = -t\sum_{z,k,\sigma}(c^\dagger_{z,k,\sigma}c_{z+1,k,\sigma}e^{ik} + c^\dagger_{z,k,\sigma}c_{z-1,k,\sigma}e^{ik} + \text{H.c.}) + \sum_{z,k,\sigma}(Fz-\mu)c^\dagger_{z,k,\sigma}c_{z,k,\sigma}$$
$$-\sum_{z,k}(\Delta^z c^\dagger_{z,-k,\downarrow}c^\dagger_{z,k,\uparrow} + \Delta^{z*}c_{z,k,\uparrow}c_{z,-k,\downarrow}) - U\sum_{z,k}(\rho^z_\uparrow c^\dagger_{z,k,\downarrow}c_{z,k,\downarrow} + \rho^z_\downarrow c^\dagger_{z,k,\uparrow}c_{z,k,\uparrow})$$
$$= \sum_k \Psi^\dagger_k\mathcal{M}(k)\Psi_k + L_w\sum_z(U\rho^z_\uparrow\rho^z_\downarrow + |\Delta^z|^2/U) + L_w\sum_z(Fz-\mu-U\rho^z_\uparrow)$$

$$\mathcal{M}(k) = \begin{pmatrix}\mathcal{T}(k) & \mathcal{D}\\ \mathcal{D}^* & -\mathcal{T}^\mathsf{T}(-k)\end{pmatrix},$$

$$\mathcal{T}(k) = \begin{pmatrix} & & \ddots & & & & & & \\ \cdots & 0 & -2t\cos(k) & -F-\mu-U\rho^{z=-1}_\downarrow & -2t\cos(k) & 0 & \cdots & & \\ & \cdots & 0 & -2t\cos(k) & -\mu-U\rho^{z=0}_\downarrow & -2t\cos(k) & 0 & \cdots & \\ & & \cdots & 0 & -2t\cos(k) & F-\mu-U\rho^{z=1}_\downarrow & -2t\cos(k) & 0 & \cdots \\ & & & & & & \ddots & & \end{pmatrix},$$

$$\mathcal{D} = \text{diag}(\Delta^{z=-L_{\max}},\ldots,\Delta^{z=-1},\Delta^{z=0},\Delta^{z=1},\ldots,\Delta^{z=L_{\max}}), \tag{5}$$

the last term in the Hamiltonian results from anti-commutation relations, $\Psi^\dagger_{z,k}$ is the Nambu spinor and the matrix $\mathcal{M}(k)$ is the Bogoliubov–de Gennes Hamiltonian.

$2L_{\max}+1$ is the total number of sites in the $\mathbf{e_z}$ direction. In the absence of interaction, we obtain $2L_{\max}+1$ one-dimensional flat bands along the $\mathbf{e_w}$ direction, each labeled by index $z$, for any finite value of $F$. The wave functions of the flat band eigenstates are superexponentially localized, and can be expressed analytically via Bessel functions. In the case where the DC field is oriented along the main diagonal, the extents of the wavefunction in the $\mathbf{e_w}$ and $\mathbf{e_z}$ directions are the same [38]. For a particle at $(z=0, w=0)$,

$$\Psi(z=0,r_w) = J_{-r_w}\left(-\frac{2t}{F}\right)J_{-r_w}\left(\frac{2t}{F}\right),$$
$$\Psi(r_z,w=0) = J_{-r_z}\left(-\frac{2t}{F}\right)J_{r_z}\left(\frac{2t}{F}\right), \tag{6}$$

where $r_w$ and $r_z$ are integers indexing the number of sites away from the center, and $J_n(x)$ are Bessel functions of the first kind and decay at least as a factorial, $1/n!$, which is faster than exponential. In the limit $L_{\max}\to\infty$, $F\neq 0$, there

will be an infinite number of flat bands labeled by $z$ in the $w$ direction. Each flat band corresponds directly to sites with equal $z$ coordinates, where consecutive flat bands have a gap of $E_{\rm gap} = F$. However, in real systems, and computationally, $L_{\rm max}$ would be finite, resulting in dispersive bands near the edges $z = \pm L_{\rm max}$, as shown in Fig. 2. In order to characterize accurately flat band superconductivity, these dispersive bands have to be fully occupied or empty.

Similarly, in 3D systems, one can orient the DC field along commensurate directions, and obtain flat bands in the planes perpendicular to it. Here, we consider the cubic lattice with a DC field of strength $E$ in the $\mathbf{e}_\gamma$ direction, and define the orthonormal vectors

$$\mathbf{e}_\alpha = \frac{1}{\sqrt{2}}\begin{pmatrix}-1\\1\\0\end{pmatrix}, \quad \mathbf{e}_\beta = \frac{1}{\sqrt{6}}\begin{pmatrix}-1\\-1\\2\end{pmatrix}, \quad \mathbf{e}_\gamma = \frac{1}{\sqrt{3}}\begin{pmatrix}1\\1\\1\end{pmatrix} \tag{7}$$

as the new basis. We can then express the mean-field Hamiltonian in momentum space,

$$\begin{aligned} 6(H-\mu N) =& -t\sum_{k_\alpha,k_\beta,\gamma,\sigma} c^\dagger_{k_\alpha,k_\beta,\gamma,\sigma}c_{k_\alpha,k_\beta,\gamma+1,\sigma}[2\cos(k_\alpha)e^{-ik_\beta}+e^{i2k_\beta}]+\text{H.c.} \\ &+\sum_{k_\alpha,k_\beta,\gamma,\sigma}\left(\frac{aE\gamma}{\sqrt{3}}-\mu\right)c^\dagger_{k_\alpha,k_\beta,\gamma,\sigma}c_{k_\alpha,k_\beta,\gamma,\sigma} - U\sum_{k_\alpha,k_\beta,\gamma}(\rho^\gamma_\uparrow c^\dagger_{k_\alpha,k_\beta,\gamma,\downarrow}c_{k_\alpha,k_\beta,\gamma,\downarrow}+\rho^\gamma_\downarrow c^\dagger_{k_\alpha,k_\beta,\gamma,\uparrow}c_{k_\alpha,k_\beta,\gamma,\uparrow}) \\ &-\sum_{k_\alpha,k_\beta,\gamma}(\Delta^\gamma c^\dagger_{k_\alpha,k_\beta,\gamma,\downarrow}c^\dagger_{-k_\alpha,-k_\beta,\gamma,\uparrow}+\Delta^{\gamma*}c_{k_\alpha,k_\beta,\gamma,\uparrow}c_{-k_\alpha,-k_\beta,\gamma,\downarrow})+L_\alpha L_\beta\sum_\gamma\left(U\rho^\gamma_\uparrow\rho^\gamma_\downarrow+\frac{|\Delta^\gamma|^2}{U}\right), \end{aligned} \tag{8}$$

where $-L_{\rm max} \leqslant \gamma \leqslant L_{\rm max}$, $\gamma \in \mathbb{Z}$, giving rise to $2L_{\rm max}+1$ quasi-two-dimensional flat bands in the tight-binding description shown in Fig. 2. Factor 6 is due to the sites in the new basis that do not exist originally. In the 3D system, the flat bands are labeled with $\gamma$.

To characterize the superconducting state, we calculate the pairing order parameter $\Delta^z/U$ in 2D ($\Delta^\gamma/U$ in 3D), the superfluid weight and the single-particle Green's function. The set of mean-field parameters, $\rho^{z(\gamma)}$ and $\Delta^{z(\gamma)}/U$, in the presence of interaction are obtained by iteratively solving the self-consistent equations (Appendix A).

The superfluid weight, $D_s$, at $T = 0$ is calculated by applying a phase twist $\Phi$ (Appendix B) in the direction perpendicular to the DC field,

$$\begin{aligned} D_s(\text{q1D}) &= \pi L_w \left.\frac{d^2E_{\rm GS}}{d\Phi^2}\right|_{\Phi=0}, \\ D_s(\text{q2D}) &= \pi \left.\frac{d^2E_{\rm GS}}{d\Phi^2}\right|_{\Phi=0}, \end{aligned} \tag{9}$$

where the (q1D) indicates the quasi-one-dimensional system, and (q2D) the quasi-two-dimensional one. $E_{\rm GS}$ is the ground state energy [43–45]. Note, $D_s = \pi\sum_{z(\gamma)}\rho_s^{z(\gamma)}$, where $\rho_s^z$ ($\rho_s^\gamma$) is the superfluid number density in the one-dimensional (two-dimensional) flat band $z$ ($\gamma$). While results are presented for both systems, we focus our analysis on the 2D (quasi-1D) Wannier-Stark lattice.

Mean-field calculations can also accurately provide information about the single-particle correlation function along and perpendicular to the field in the presence of interactions, with

$$\begin{aligned} G_\sigma(r_w) &= \langle c_{z,w,\sigma}c^\dagger_{z,w+r_w,\sigma}\rangle, \\ G_\sigma(r_z) &= \langle c_{z,w,\sigma}c^\dagger_{z+r_z,w,\sigma}\rangle, \end{aligned} \tag{10}$$

where $r_w, r_z \in \mathbb{Z}$, and we compute these quantities for the 2D Wannier-Stark lattice to obtain insights about the spatial extent of the Cooper pairs [46].

In this study, we choose $\mu = -\frac{U}{2}$ to obtain a half-filled $z = 0$ ($\gamma = 0$ in 3D) flat band, and choose sufficiently large $L_{\rm max}$, such that all dispersive bands due to finite size effects are either completely full or empty. All energies are measured in the units of the hopping potential $t = 1$, the lattice constant is fixed at $a = 1$, and the temperature is $T = 0$.

## III. RESULTS AND DISCUSSION

### A. 2D square lattice

We define $F = \frac{aE}{\sqrt{2}}$ for the square lattice with the DC field of strength $E$ along the main diagonal. In the presence of a DC field, $E_{\rm gap} = F$. As we increase $F$, energy gaps between neighboring diagonals become bigger and the wave functions are increasingly localized in real space. With the interplay between the DC field strength and attraction, we find a strong dependence of the $z$-band filling and the pairing order parameter on these parameters.

The first ingredient for superconductivity is the existence of the Cooper pairs, quantified by the pairing order parameter, $\Delta^z/U$, and the single-particle correlation length, $\xi$, characterizing the spatial extent of the pair. For dispersive bands in 2D, the critical temperature of pairing is of the order of $k_BT_c \sim \Delta(T=0) \sim e^{-a/U}$, but it has been shown that $k_BT_c \sim \Delta(T=0) \sim U$ for flat bands [7,8,14,15,17,20]. We show in Figs. 3 and 4 the $z$-band filling, $\rho^z$, and pairing order parameter, $\Delta^z/U$, at $F = 0.5$ and $F = 1$, with a range of attraction strengths $0.1 \leqslant U \leqslant 7$. While the filling on the $z = 0$ band is $\rho^{z=0} = 0.5$ for all values of $U$ and $F$ (as per our choice of the chemical potential), the spread of partially filled bands ($0 < \rho^z < 1$) narrows with increasing DC field and attraction strength (Fig. 3). Since $\Delta^z/U$ is nonzero only for bands with partial filling, the number of bands with finite and large $\Delta^z/U$

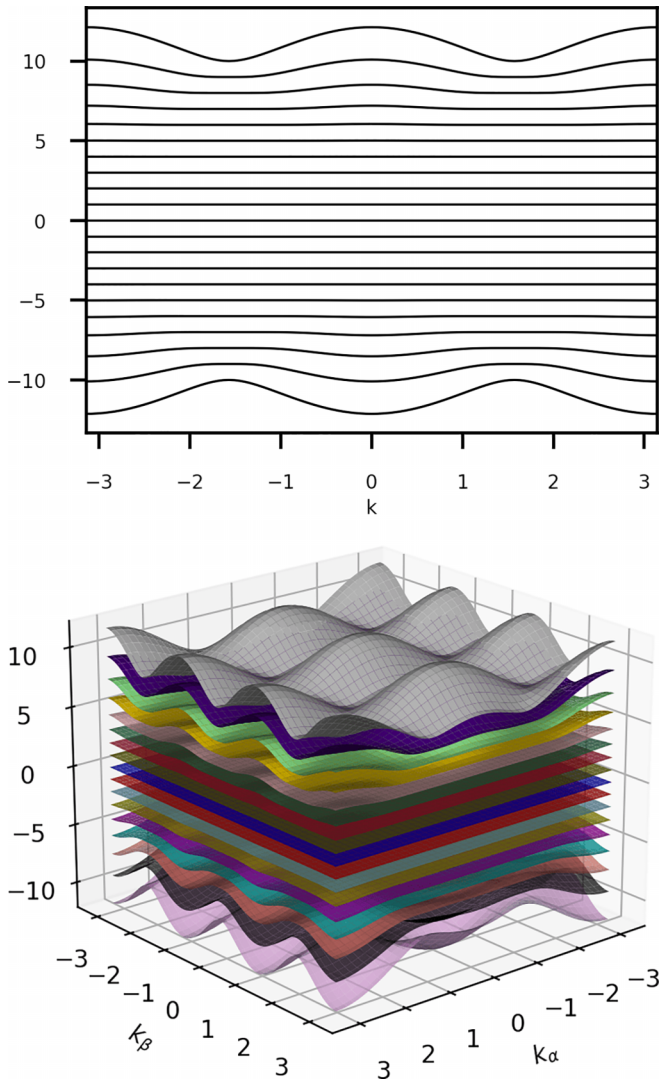


FIG. 2. $D-1$ Wannier-Stark flat bands with finite a $L_{\max}$. Bands acquire finite dispersion at the edges of the spectrum due to finite size effects. Top: The 2D square lattice with $F=1$. Bottom: The 3D cubic lattice with $F=1$.

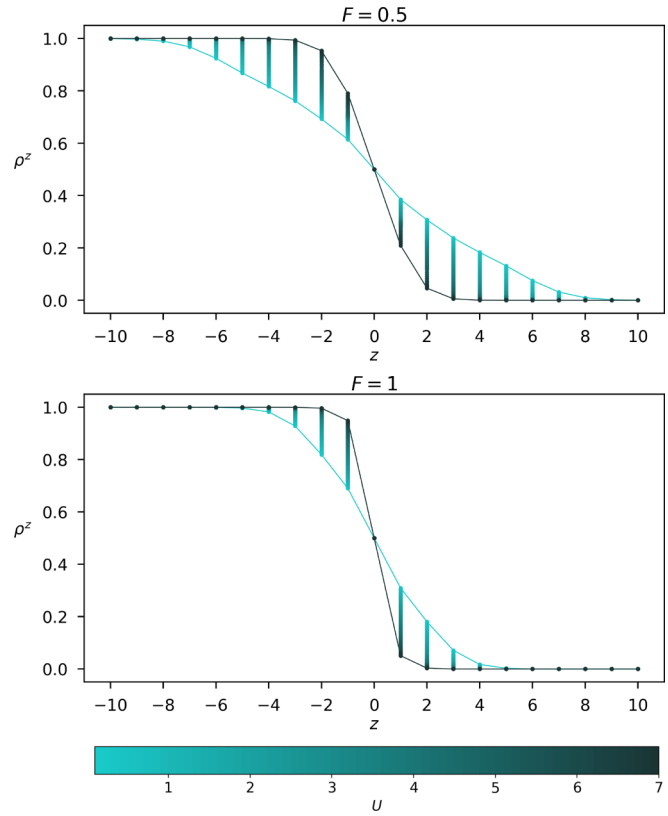


FIG. 3. Values of $z$-band filling, $\rho^z$, for $0.1 \leqslant U \leqslant 7$ with (top) $F=0.5$ and (bottom) $F=1$, where light (dark) color represents weaker (stronger) interaction strength. Solid lines are shown for $U=0.1$ and $U=7$. Since we have equal populations for the up and down spins, $\rho^z_\uparrow = \rho^z_\downarrow = \rho^z$. $z$-bands with $0 < \rho^z < 1$ are partially filled, and $\rho^{z=0} = 0.5$ for all values of $U$. Due to the larger energy gap between the flat bands as $F$ increases, the number of partially filled bands decreases. With stronger attractive interaction, the number of bands with partial filling also decreases.

also decreases, as is evident in the narrowing peak about $z=0$ in Fig. 4. Due to the larger band gap and the faster decay of the wave function as $F$ increases, the number of partially filled $z$ bands decreases, even at finite interaction. On the other hand, as $U$ increases, the Cooper pairs are more tightly bound, increasing the $\Delta^{z=0}$ peak, but narrowing the spread of the wave function in the $\mathbf{e_z}$ direction.

For these values of the DC field, $F=0.5$ and $F=1$, the pairing order parameter, $\Delta^{z=0}/U$, on the half-filled band is finite for any weak interaction and increases with $|U|$, which is usually observed for interacting flat band systems [2]. In contrast to dispersive bands, in flat band systems *with CLS*, the Cooper pair sizes are smaller than a single lattice spacing [2,3] for *any* value of $U$, thus there is no BCS-BEC crossover, and the pairing order parameter remains large even for weak interaction. However, here, as both the DC field and $U$ are further decreased, the pairing order parameter is substantially suppressed (Fig. 5). In the limit $F \to 0$, the pairing order parameter of the half-filled square lattice with a dispersive band is recovered on the $z=0$ flat band, as the single particle wave function is increasingly spread out across the square lattice, even in the presence of a DC field.

This is an interesting feature of Wannier-Stark flat bands that is distinct from flat bands with CLS, and can be understood as follows. As $F$ is decreased, the wave function becomes less localized, while the existence of flat bands persists. Figure 6 (top) shows the single-particle correlation function as a function of distance along the flat band at $z=1$ [47], i.e., transverse to the field, and (bottom) the correlation length for various values of $U$ and $F$. It is clear in the top panel that this correlation function decays exponentially, $G_\sigma(r_w) \sim e^{-r_w\sqrt{2}/\xi}$, thus yielding the correlation length, $\xi$, which characterizes the size of the pair. The $\sqrt{2}$ factor in the exponent arises from the distance between consecutive sites in the $\mathbf{e_w}$ direction. At fixed $F$, the decay is faster for larger $U$, resulting in smaller pairs with smaller values of $\xi$. The bottom panel of Fig. 6 shows the correlation length in the $\mathbf{e_w}$ direction as a function of $F$ and $U$. It is clear, then, that at small values of $U$ and $F$ the correlation length exceeds the lattice spacing, and that, therefore, the pair extends over several unit cells in

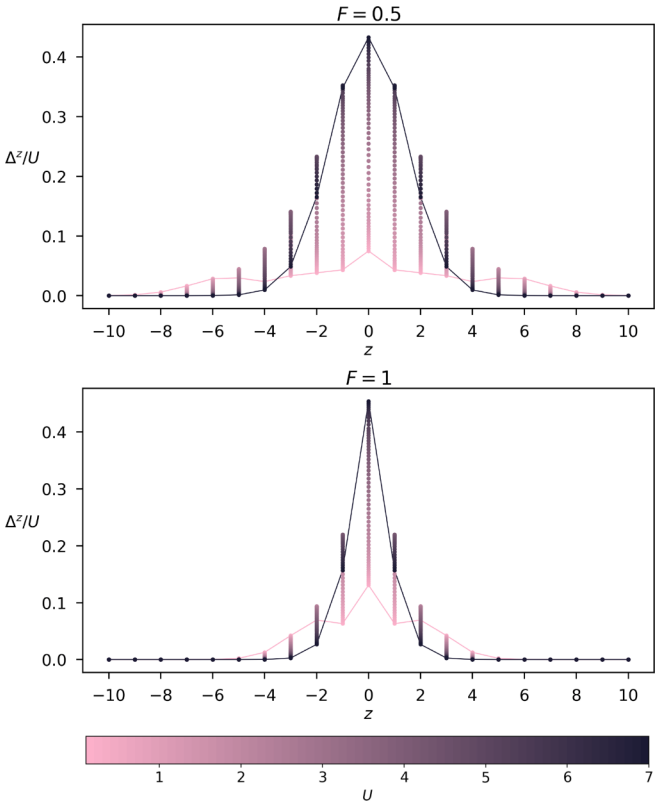


FIG. 4. Values of $\Delta^z/U$ for $0.1 \leqslant U \leqslant 7$ with (top) $F = 0.5$ and (bottom) $F = 1$, where light (dark) colors represent weaker (stronger) interaction strength. Lines are shown for $U = 0.1$ and $U = 7$. $\Delta^z(z = 0)/U$ increases with stronger interaction. Additionally, the spread becomes narrower as $F$ and the band gap increase, corresponding directly to the partially filled bands in Fig. 3.

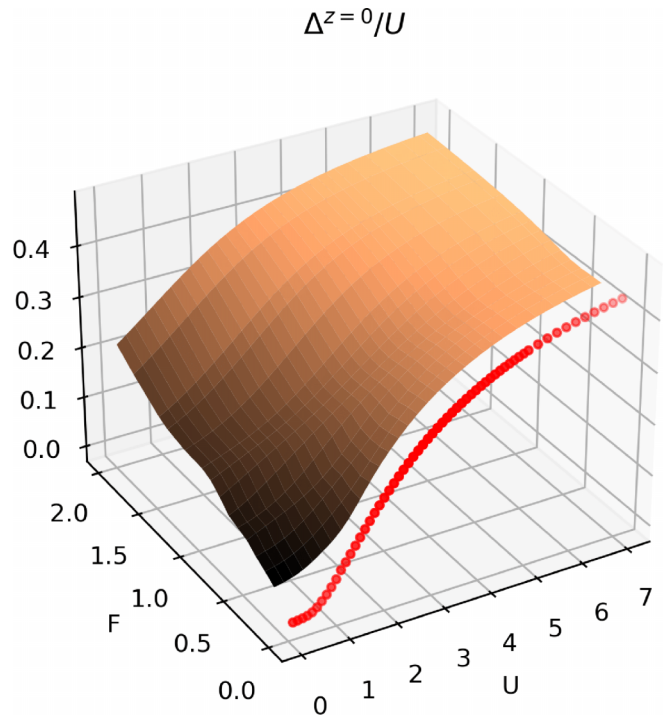


FIG. 5. The values of $\Delta^{z=0}/U$ on the half-filled $z = 0$ band as a function of $F$ and $U$. The red points are $\Delta/U$ of the half-filled square lattice with a dispersive band, when $F = 0$.

the transverse direction. In addition, as $F$ and/or $U$ decrease, the pair wave function also spreads out along the direction of the DC field, $\mathbf{e_z}$ as seen in Fig. 7. However, the decay of the wave function in the direction of the DC field is faster than exponential and is essentially given by a rescaling of the $U = 0$ wave function, Eq. (6). This spread of the wave function along $\mathbf{e_z}$ and $\mathbf{e_w}$ as $F$ and $U$ decrease causes the order parameter, $\Delta^z/U$, to decrease as seen in Fig. 5.

It is interesting to elaborate some more on the behavior of the correlation functions along and transverse to the applied DC field as $F$ or $U$ decrease. First, we emphasize that, for any nonzero value of $F$, the flat bands exist. At $U = 0$, the wave function is given by Eq. (6) and is the same along and transverse to the applied DC field: it spreads isotropically as $F$ decreases, and it decays faster than exponentially. When $U > 0$, the wave function becomes a scaled Bessel function in the direction of the applied field, as seen in Fig. 7, and therefore still decays faster than exponentially. However, in the transverse direction it decays exponentially (Fig. 6). Fixing $U$ at a small value and calculating $\xi$ as a function of $F$, we find that $\xi$ increases rapidly as $F$ decreases, Fig. 6 (bottom). We show in Fig. 8 (right) a cut along $U = 1$ demonstrating this rapid increase which appears to be a power law divergence $\xi \sim 1/F$. Going to an even smaller values of $F$ was too challenging, since it required extremely large system sizes. On the other hand, fixing $F$ at some small value and taking $U \to 0$, the behavior is different: at first $\xi$ increases, but then eventually it decreases, Fig. 8 (left). This is because, as $U$ vanishes, the wave function reverts to its noninteracting limit and decays faster than exponentially in all directions.

The second essential ingredient for superconductivity is for the pairs to exhibit phase stiffness which is manifested by nonzero superfluid weight, Eq. (9). The spread of the single-particle flat band wave functions, causing an increase of overlap of the wave functions of the particle population, was previously found to have direct implications on the superfluid weight when $U \neq 0$ [3,6]. We therefore investigate the dependence of $D_s$ on $F$ and $U$.

We observe in Fig. 9 (and Fig. 13 in Appendix B) that for each value of $F$ the superfluid weight at first increases linearly with $U$, reaches a peak at around $U \approx 2$, and then decreases. The linear dependence on $U$, for small $U$, has been previously shown to be caused by the flat band, with nonzero minimal quantum metric [3,5,6,48,49]. Note that in these cases the CLS wave function covers more than one unit cell. For quasi-one-dimensional non topological bands, i.e., with vanishing minimal quantum metric, the CLSs are localized within one unit cell, resulting in a suppression of superfluid transport leading to $D_s \propto U^\alpha$ with $\alpha > 2$. Interestingly, the quasi-one-dimensional flat bands in our case, resulting from the applied DC field, are nontopological, i.e., with vanishing quantum metric, yet yield $D_s \propto U$ for small $U$. The reason for this is that in the current system the localized state is not compact: the wave function, Eq. (6), extends over more than one unit cell and results in nonzero overlap between the wave functions of the particle population, which then can lead to

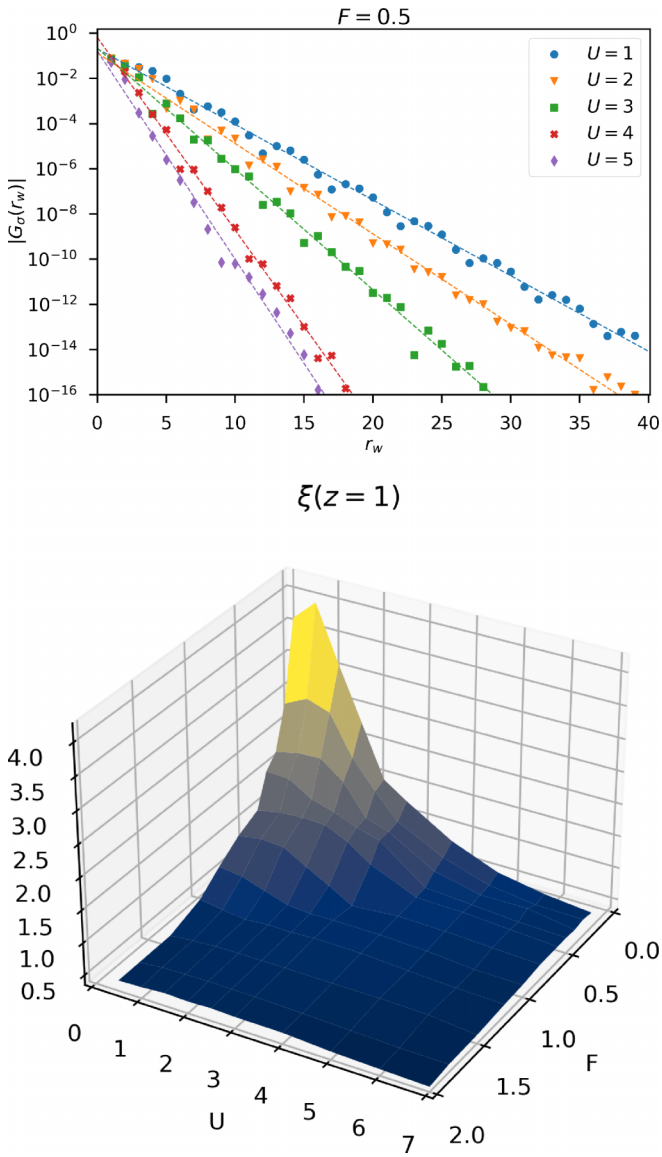


FIG. 6. Top: Correlation function on the 2D Wannier-Stark lattice decays exponentially along the $\mathbf{e_w}$ direction, shown for $F = 0.5$. Bottom: Correlation length as a function of $U$ and electric field strength in the $\mathbf{e_w}$ direction. For sufficiently strong DC fields ($F > 1$), the correlation length saturates to a value less than one lattice spacing as $U \to 0$.

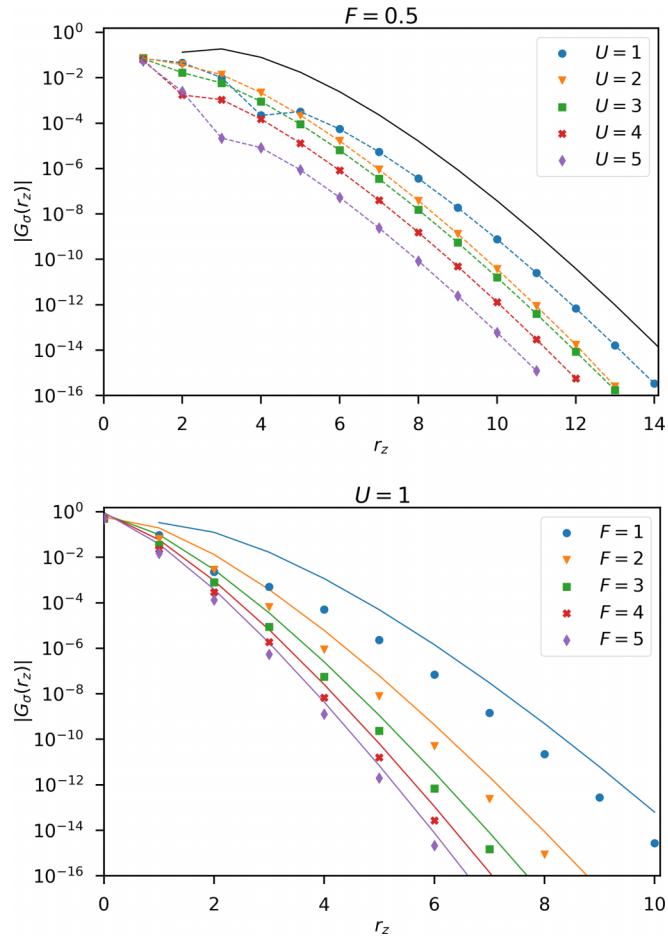


FIG. 7. The correlation function on the 2D Wannier-Stark lattice in the $\mathbf{e_z}$ direction, $|G_\sigma(r_z)|$. Top: At $F = 0.5$ and several $1 \leqslant U \leqslant 5$. The black solid line is the noninteracting wave function at $F = 0.5$, $\Psi(r_z, w = 0) = J_{-r_z}(-4)J_{r_z}(4)$ [see Eq. (6)]. Bottom: At $U = 1$ and several $1 \leqslant F \leqslant 5$. The solid lines correspond to the noninteracting wave functions as defined in Eq. (6).

a linear dependence on $U$. At very large $U$, the physics is very well described by an effective extended hard-core Bose-Hubbard model which exhibits a decreasing $D_s$ as $U$ increases [2,3,16,49,50]. These two branches of $D_s$, linear increase at low $U$ and decrease at large $U$, meet in the intermediate $U$ regime where the physics is dominated by band mixing and $D_s$ displays a maximum.

We expect this maximum value to be of the order of the relevant band width of the unbiased noninteracting lattice which is proportional to the hopping $t = 1$. For a fixed nonzero DC field value, the single-particle wave function extension along the $z$ direction is proportional to $\frac{t}{F}$. Let us assume that $F < t$, which corresponds to the most interesting regime of large superfluid weight. For $U < F$ we expect very weak superfluid

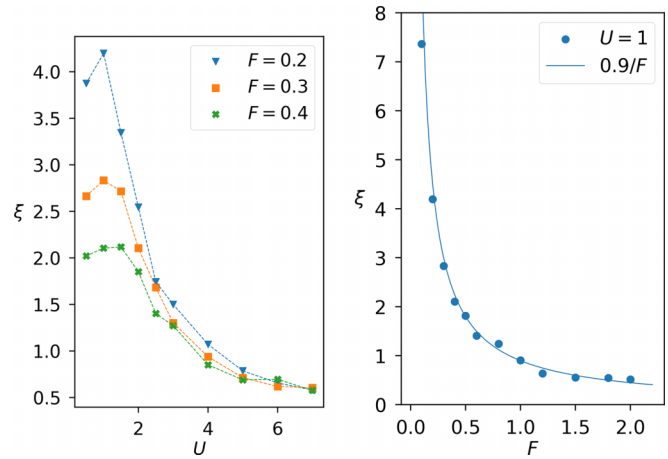


FIG. 8. Correlation length along the $\mathbf{e_w}$ direction on the 2D Wannier-Stark lattice. Left: Fixed $F$ as a function of $U$ for three values of $F$. The lines are included to guide the eye. Right: Fixed $U$ as a function of $F$.

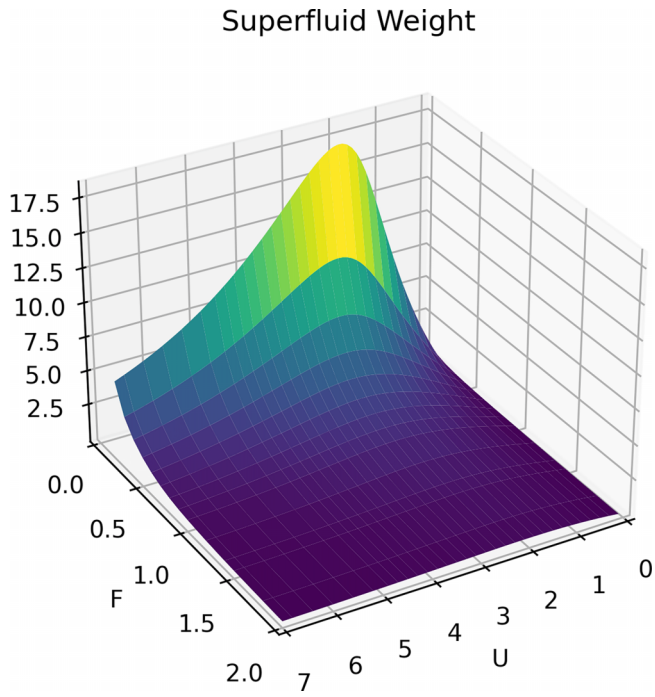


FIG. 9. Superfluid weight on the 2D Wannier-Stark lattice along the $\mathbf{e_w}$ direction as a function of DC field and Hubbard interaction strengths. (Details in Appendix B.)

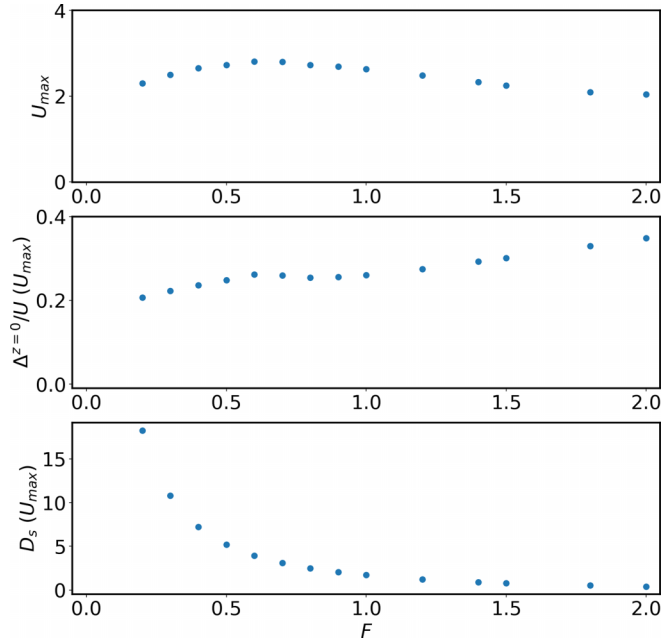


FIG. 10. Top: The value of $U_{\max}$ corresponding to the peak in $D_s$ as a function of $F$. Middle: Pairing order parameter at $U_{\max}$ as a function of $F$. Bottom: The maximum attainable superfluid weight as a function of $F$.

features, as discussed above. Increasing $U$ will couple more and more flat bands and thus increase the superfluid weight. When $U$ reaches a value around $U \sim t$ all bands within the reach of one eigenfunction extent along the $z$ direction are coupled. Further increase of $U$ will not lead to a further increase of the weight, but instead lead smoothly into the regime of hard core bosons, which means instead a decrease of the superfluid weight. Therefore, $U_{\max} \sim t$, and we can expect that the value of the superfluid weight at the maximum will increase as $F$ is further decreased since more and more flat bands participate. For the case $F > t$, we expect $U_{\max} \to 0$ and a suppression of superfluidity with increasing $F$, since the density overlap between localized flat band states will quickly decrease.

Remarkably, as the strength of the DC field is decreased, the superfluid weight is enhanced dramatically, unlike the pairing order parameter, $\Delta^z/U$, which decreases as discussed above. This enhancement of $D_s$ can be understood as follows: The wave function asymptotics of this Wannier-Stark system in the noninteracting limit is [38]

$$|\Psi(r_z, w = 0)| \approx \frac{1}{|r_z|!^2} \left|\frac{t}{F}\right|^{2|r_z|}. \tag{11}$$

Since any finite DC field breaks the periodicity in the $\mathbf{e_z}$ direction, a weak DC field produces multiple flat bands in the $\mathbf{e_w}$ direction with diminished gaps of $E_{\text{gap}} = F$ between consecutive $z$ bands. Additionally, the wave function in the $\mathbf{e_z}$ direction broadens $\sim\frac{t}{F}$, directly increasing the number of partially filled $z$ bands which can participate in supercurrent transport. Consequently, as $F$ becomes smaller, but nonzero, the flat bands become more closely packed, and more of them are covered by the spreading wave function and are doped (see Fig. 3). This results in the observed improvement of $D_s$. Note that $F$ can be very small but cannot be zero: When $F = 0$, the system reverts to the usual single (dispersive) band Hubbard model. We emphasize that while the pairing order parameter is a local quantity and converges to the dispersive square lattice limit as $F \to 0$ and the wave function spreads, the superfluid weight describes the dissipationless transport of the entire system and depends on the number of bands contributing to flat band superconductivity. Moreover, the system is effectively quasi-one-dimensional in the presence of a DC field, thus the square lattice limit of $D_s$ will *not* be recovered even as $F \to 0$, and is in fact dramatically enhanced with a weak DC field strength.

It is interesting to study the dependence of the maximum attainable superfluid weight, $D_s$, as a function of the DC field strength. We observe in Fig. 10 that the interaction strength and pairing order parameter which correspond to the maximum $D_s$ do not vary significantly as the DC field strength is changed. As previously explained, $U_{\max}$ is attained when all partially filled bands are coupled, at $U \sim t$. However, due to the increasing spread of the wave function and narrowing of band gaps, the maximum $D_s$ grows and diverges as $F \to 0$.

For superconductivity to remain robust at finite temperature, both $D_s$ and $\Delta^z$ need to be nonzero and large. A large $D_s$ means more carriers to participate in the supercurrent. Since $\Delta^z$ is the energy to break a pair (the spin gap), the larger its value the higher the critical temperature, $T_c \sim \Delta^z$. We see in Fig. 10 that the maximum $D_s$ is obtained for $2 \lesssim U_{\max} \lesssim 3$, and at the same time $\Delta^z/U_{\max} > 0.2$ as $F$ is varied. In other words, the critical temperature, $T_c \sim \Delta^z \gtrsim 0.4$ remains roughly constant as $F$ is decreased while $D_s(U_{\max})$ increases rapidly. Therefore, superconductivity is much enhanced at small but nonzero $F$.

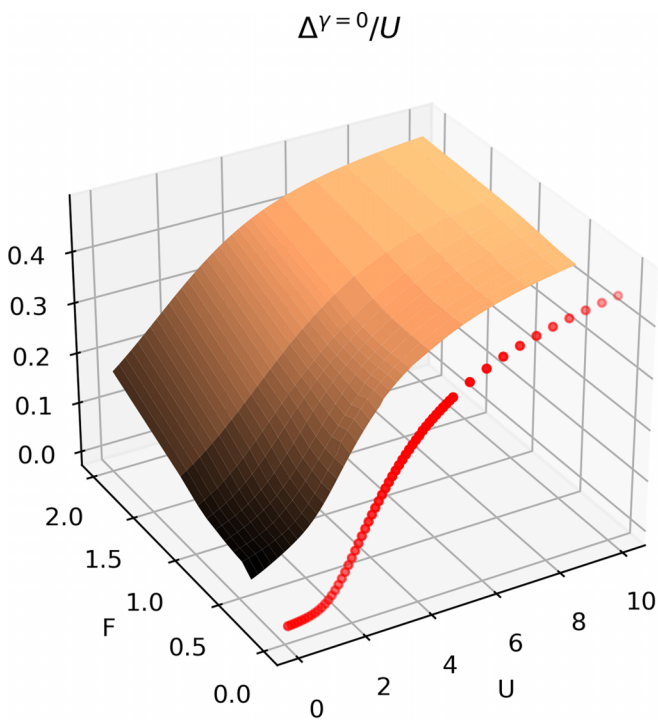


FIG. 11. The pairing order parameter $\Delta^{\gamma=0}/U$ as a function of the DC field and interaction strengths on the half-filled $\gamma = 0$ band for the cubic lattice. The red points are the pairing order parameter on a half-filled cubic lattice with a dispersive band, when $F = 0$.

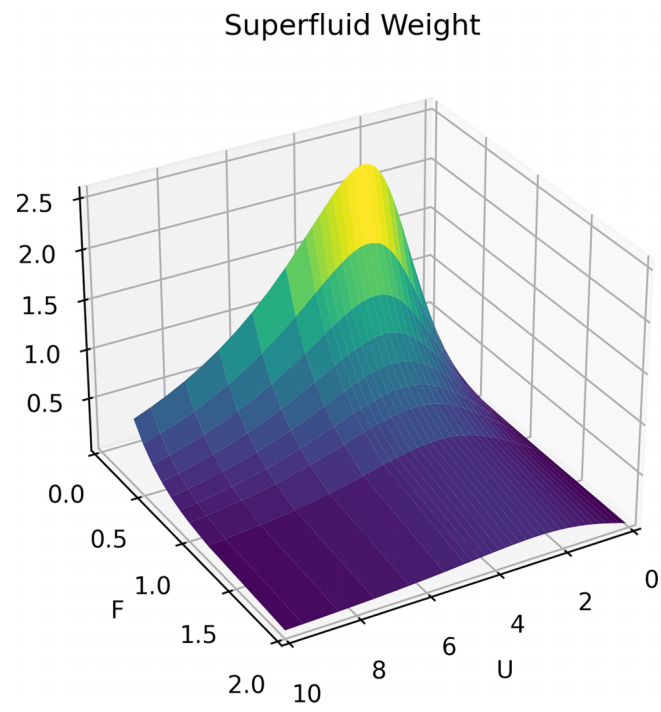


FIG. 12. The superfluid weight perpendicular to $\mathbf{e}_\gamma$ in the 3D Wannier-Stark lattice as a function of $U$ and $F$. (Details in Appendix B.)

### B. 3D cubic lattice

For completeness, we extend the study to the 3D Wannier-Stark lattice defined in Eq. (8). By applying a DC field in the $\mathbf{e}_\gamma$ direction, we have $F = \frac{aE}{\sqrt{3}}$ with $E$ the DC field strength. The flat bands which result are perpendicular to $\mathbf{e}_\gamma$ and have an energy gap of $F$ between consecutive planes (Fig. 2). Here, the $\gamma = 0$ band is fixed at half filling.

Overall the results are similar to the 2D case. As before, we observe a decrease of the pairing order parameter, $\Delta^{\gamma=0}/U$, as both the DC field $F$ and attraction strengths $U$ decrease, due to the delocalization of the single particle wave function as $F$ is tuned to zero. However, at weak interaction, we still have a large and finite value for sufficiently strong $F$ (Fig. 11). In the limit $F \to 0$, we recover the pairing order parameter of the cubic lattice shown in red points in Fig. 11.

Figure 12 illustrates the dependence of superfluid weight, $D_s$, on the DC field and interaction strength for the 3D Wannier-Stark lattice. Again, there is a strong enhancement of $D_s$ when the DC field strength is weak, which produces multiple partially filled flat bands with small band gaps.

## IV. CONCLUSIONS

In this study, we characterize in detail the superconducting properties of interacting fermions in Wannier-Stark flat band lattices obtained by applying a DC field along a diagonal of the square lattice. Superconducting transport has two main ingredients: the formation of Cooper pairs which become a condensate (or quasi-condensate) and their nonzero superfluid weight due to the phase stiffness of pairs. We calculated the pairing order parameter, correlation functions, and the superfluid weight while systematically varying the DC field and interaction strength, and uncovered the dependence of the superconducting properties on these parameters.

We showed that, unlike flat band systems with a compact localized state, CLS, here transport is supported cooperatively by multiple flat bands as the spatial extent of the wave function spreads across several $z$ coordinates corresponding directly to flat $z$ bands (or $\gamma$ bands in 3D). Therefore, the physics is different from flat band systems with CLS and nonzero minimal quantum metric where superconductivity at weak interaction is governed by the eigenstates and quantum geometry of the flat band. Despite the trivial topology of this system, we have demonstrated that it supports flat band superconductivity due to the noncompact nature of the localized state. Furthermore, the superconductivity can be enhanced easily on these Wannier-Stark flat bands by tuning the amplitude of the applied DC field. Reducing the DC field strength increases the number of partially-filled flat band channels that contribute towards superconductivity and the overlap of the single-particle wave functions.

The results presented would be qualitatively similar for any commensurate direction that the DC field is oriented in, and on all Wannier-Stark flat band systems, independently of the underlying Bravais lattice. We propose that the experimental realization of Wannier-Stark flat band systems is advantageous as they require less fine tuning but can similarly result in flat band superconductivity. For example, it is possible to study this system in experiments with ultracold atoms loaded in optical lattices. In this situation, the DC field is emulated by the gravitational field when the lattice is tilted at an angle [39–42]. Moreover, there is no CLS, and the density overlap

of the noninteracting wave functions can be controlled with the DC field strength, which increases the coherent transport of the Cooper pairs.

It would be insightful to analyze the many-body interactions and superconducting properties on non-Bravais Wannier-Stark lattices and topological flat Wannier-Stark bands, like the ones proposed in Refs. [51] and [52]. Since the effective dimension of the superconducting channel is $D-1$, it would also be interesting to explore the effect of disorder on Wannier-Stark flat bands.

## ACKNOWLEDGMENTS

S.M.C. is supported by a National University of Singapore President's Graduate Fellowship and the Center for Theoretical Physics of Complex Systems, Institute for Basic Science (PCS-IBS) Visitors Program. S.M.C. would like to thank PCS-IBS in the Republic of Korea for their kind hospitality and stimulating research environment. A.A. and S.F. acknowledge financial support from the Institute for Basic Science (IBS) in the Republic of Korea through the Project No. IBS-R024-D1.

## APPENDIX A: MEAN-FIELD APPROXIMATION ON WANNIER-STARK FLAT BANDS

To derive the mean-field expression of the interaction term in Eq. (4) of the main text, we first recognize that sites on equivalent $z$ bands are identical, but the mean field parameters should depend on the index $z$. In other words, the pairing and filling on different $z$ bands should be distinct. We can then write a trial Hamiltonian for the interaction part,

$$H_{I,\text{trial}} = -\frac{1}{2}\sum_{z,w}(\Delta^z c^\dagger_{z,w,\downarrow}c^\dagger_{z,w,\uparrow} + \Delta^{z*}c_{z,w,\uparrow}c_{z,w,\downarrow}) - \frac{U}{2}\sum_{z,w}(\rho^z_\uparrow c^\dagger_{z,w,\downarrow}c_{z,w,\downarrow} + \rho^z_\downarrow c^\dagger_{z,w,\uparrow}c_{z,w,\uparrow}) \quad \text{(A1)}$$

with the mean-field parameters $\Delta^z/U$, $\rho^z_\uparrow$, $\rho^z_\downarrow$ to be defined.

We write the Gibbs-Bogoliubov inequality at $T=0$ [53],

$$\langle H_I\rangle \leqslant -\frac{U}{2}\sum_{z,w}\langle c^\dagger_{z,w,\uparrow}c_{z,w,\uparrow}c^\dagger_{z,w,\downarrow}c_{z,w,\downarrow}\rangle_{\text{trial}} + \frac{1}{2}\sum_{z,w}\langle(\Delta^z c^\dagger_{z,w,\downarrow}c^\dagger_{z,w,\uparrow} + \Delta^{z*}c_{z,w,\uparrow}c_{z,w,\downarrow})\rangle_{\text{trial}} + \frac{U}{2}\sum_{z,w}\langle(\rho^z_\uparrow c^\dagger_{z,w,\downarrow}c_{z,w,\downarrow} + \rho^z_\downarrow c^\dagger_{z,w,\uparrow}c_{z,w,\uparrow})\rangle_{\text{trial}} + \langle H_{I,\text{trial}}\rangle_{\text{trial}} \quad \text{(A2)}$$

where $\langle\cdots\rangle_{\text{trial}}$ denotes expectation values with respect to the weight $e^{-\beta H_{I,\text{trial}}}/Z_{\text{trial}}$. Minimizing, we obtain the mean field interaction term and the mean-field parameters,

$$\langle\widetilde{H}_I\rangle = \langle H_{I,\text{trial}}\rangle + \frac{1}{2}L_w\sum_z(U\rho^z_\uparrow\rho^z_\downarrow + |\Delta^z|^2/U),$$
$$\rho^z_\uparrow = \langle c^\dagger_{z,w,\uparrow}c_{z,w,\uparrow}\rangle,$$
$$\rho^z_\downarrow = \langle c^\dagger_{z,w,\downarrow}c_{z,w,\downarrow}\rangle,$$
$$\frac{\Delta^z}{U} = \langle c_{z,w,\uparrow}c_{z,w,\downarrow}\rangle. \quad \text{(A3)}$$

With this approximation, we can write the Hamiltonian in the Bogoliubov–de Gennes (BdG) form in reciprocal space and diagonalize,

$$2(H-\mu N) = \sum_k \Psi^\dagger_k\mathcal{M}(k)\Psi_k + \text{const} = \sum_k \Psi^\dagger_k\mathcal{P}(k)\mathbf{\Lambda}(k)\mathcal{P}^{-1}(k)\Psi_k + \text{const} = \sum_k \Gamma^\dagger_k\mathbf{\Lambda}(k)\Gamma_k + \text{const}, \quad \text{(A4)}$$

where

$$\text{const} = L_w\sum_z(U\rho^z_\uparrow\rho^z_\downarrow + |\Delta^z|^2/U + Fz - \mu - U\rho^z_\uparrow).$$

The Nambu spinor $\Psi_k$ comprising the operators $c_{z,w,\uparrow}$ and $c^\dagger_{z,w,\downarrow}$ can be identified to be

$$\Psi_k = \mathcal{P}(k)\Gamma_k, \quad \text{(A5)}$$

where $\Gamma_k$ consists of operators for quasiparticle excitation, $\gamma_n$, $n=1,2,\ldots,2L_{\max}+1$ corresponding to positive eigenvalues and $\gamma^\dagger_n$, $n=2L_{\max}+2, 2L_{\max}+3,\ldots,2(2L_{\max}+1)$ corresponding to negative eigenvalues. The columns of $\mathcal{P}(k)$ are eigenvectors, $u_n$, of $\mathcal{M}(k)$. Recognizing that there are no quasiparticle excitations in the ground state, $\langle\gamma^\dagger_n\gamma_n\rangle = 0$, the only contributing terms are $\langle\gamma_n\gamma^\dagger_n\rangle = 1$ and we can determine the mean field parameters self-consistently with the eigenvectors of the BdG Hamiltonian.

To find $\Delta^z$ and $\rho^z_\sigma$, we compute

$$\frac{\Delta^z}{U} = \frac{1}{L_w}\sum_k\sum_{n=1}^{2L_{\max}+1}u_{n,z}u^*_{n,z+2L_{\max}+1},$$
$$\rho^z_\downarrow = \frac{1}{L_w}\sum_k\sum_{n=1}^{2L_{\max}+1}|u_{n,z+2L_{\max}+1}|^2, \quad \text{(A6)}$$
$$\rho^z_\uparrow = \frac{1}{L_w}\sum_k\sum_{n=2L_{\max}+2}^{2(2L_{\max}+1)}|u_{n,z}|^2,$$

where $u_{n,m}$ is the $m$th element of eigenvector $u_n$. Since the eigenvectors are inherently dependent on the mean-field parameters which enter the BdG Hamiltonian, Eqs. (A6) are the set of self-consistent equations that have to be satisfied to find the mean-field parameters and ground state of the system.

## APPENDIX B: THE SUPERFLUID WEIGHT

To compute the superfluid weight, we determine the ground state energy in the presence of a phase twist, $\Phi$.

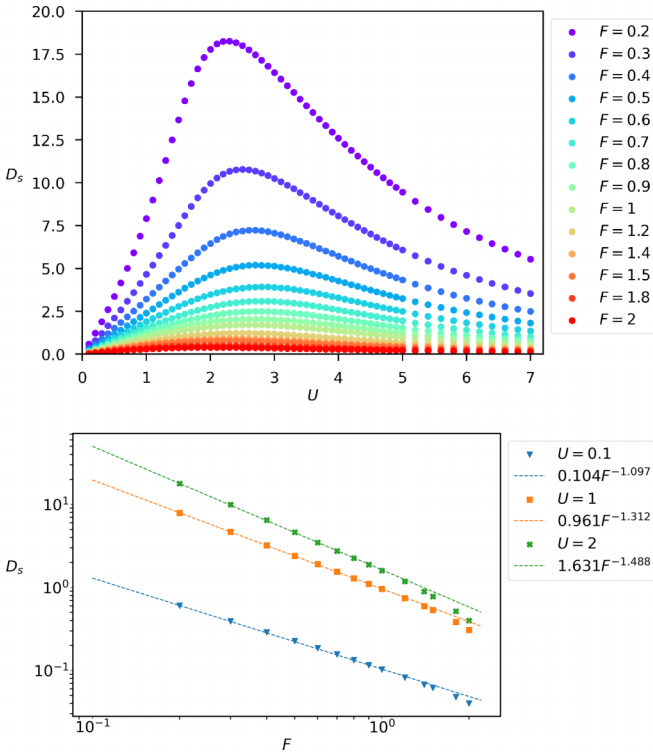


FIG. 13. Top: Superfluid weight on the 2D Wannier-Stark lattice along the $\mathbf{e}_w$ direction as a function of the attraction strength. Bottom: Superfluid weight on the 2D Wannier-Stark flat bands as a function of the DC field strength behaves as a power law at weak interaction.

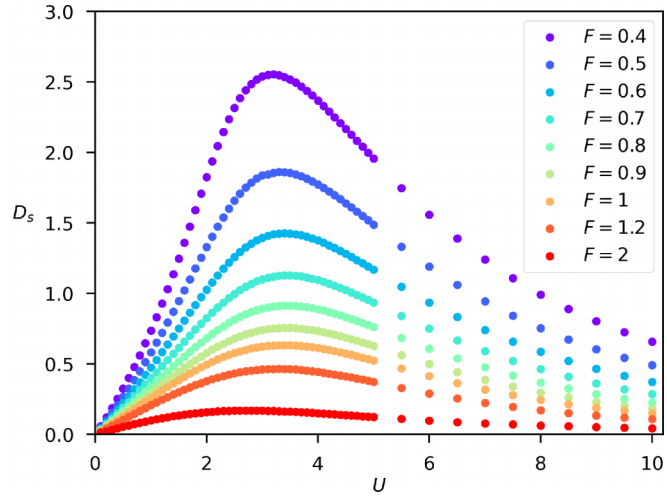


FIG. 14. Superfluid weight perpendicular to $\mathbf{e}_\gamma$ on the 3D Wannier-Stark lattice as a function of the attraction strength.

For the 2D square lattice, we apply a phase twist in the $\mathbf{e}_w$ direction to calculate the superfluid weight. Specifically, we implement a local gauge transformation on the operators, with $c_{z,w,\sigma} \to c_{z,w,\sigma} e^{iw\phi}$ and $\phi = \frac{\Phi}{\sqrt{2}L_w}$ is the phase gradient.

In the 3D case, we can choose to compute the superfluid weight in any direction, $\mathbf{e}_\delta$, where $\delta = n\alpha + m\beta$ on the 2D flat band and we replace the operator $c_{\alpha,\beta,\gamma,\sigma} \to c_{\alpha,\beta,\gamma,\sigma} e^{i\delta\phi_\delta}$. The phase gradient, $\phi_\delta$, depends on the direction we apply the phase twist; for example in the $\alpha$ direction the phase gradient is $\phi_\alpha = \frac{\Phi}{L_\alpha\sqrt{2}a}$, and in the $\beta$ direction the phase gradient is $\phi_\beta = \frac{\Phi}{L_\beta\sqrt{6}a}$. Following this procedure, the superfluid weight can be shown to be independent of the direction in which we apply the phase twist.

In the main text, we showed how the superfluid weight varies as a function of both $F$ and $U$. Here, we include cuts of the surface plot in Figs. 13 and 14 for the 2D and 3D Wannier-Stark systems respectively. For any DC field strength, the superfluid weight increases at weak interaction with transport governed by the density overlaps of the single-particle wave function on the flat bands, peaks at intermediate $U$, and decreases as the spread of the partially filled flat bands decreases at strong $U$.

Additionally, we show in Fig. 13 the power law dependence of the superfluid weight on the DC field strength, for $0.2 \leqslant F \leqslant 2$, at weak to intermediate interactions of $U = 0.1$, 1, and 2. We see that the effect of the wave function broadening as $\frac{t}{F}$ is especially evident for $U = 0.1$, where $D_s \sim F^{-1.097}$.


[1] Y. Cao, V. Fatemi, S. Fang, K. Watanabe, T. Taniguchi, E. Kaxiras, and P. Jarillo-Herrero, Unconventional superconductivity in magic-angle graphene superlattices, Nature (London) **556**, 43 (2018).

[2] S. M. Chan, B. Grémaud, and G. G. Batrouni, Pairing and superconductivity in quasi-one-dimensional flat-band systems: Creutz and sawtooth lattices, Phys. Rev. B **105**, 024502 (2022).

[3] S. M. Chan, B. Grémaud, and G. G. Batrouni, Designer flat bands: Topology and enhancement of superconductivity, Phys. Rev. B **106**, 104514 (2022).

[4] F. Xie, Z. Song, B. Lian, and B. A. Bernevig, Topology-bounded superfluid weight in twisted bilayer graphene, Phys. Rev. Lett. **124**, 167002 (2020).

[5] K.-E. Huhtinen, J. Herzog-Arbeitman, A. Chew, B. A. Bernevig, and P. Törmä, Revisiting flat band superconductivity: Dependence on minimal quantum metric and band touchings, Phys. Rev. B **106**, 014518 (2022).

[6] M. Tovmasyan, S. Peotta, P. Törmä, and S. D. Huber, Effective theory and emergent SU(2) symmetry in the flat bands of attractive Hubbard models, Phys. Rev. B **94**, 245149 (2016).

[7] S. Peotta and P. Törmä, Superfluidity in topologically nontrivial flat bands, Nat. Commun. **6**, 8944 (2015).

[8] V. Peri, Z.-D. Song, B. A. Bernevig, and S. D. Huber, Fragile topology and flat-band superconductivity in the strong-coupling regime, Phys. Rev. Lett. **126**, 027002 (2021).

[9] A. Julku, S. Peotta, T. I. Vanhala, D.-H. Kim, and P. Törmä, Geometric origin of superfluidity in the Lieb-lattice flat band, Phys. Rev. Lett. **117**, 045303 (2016).

[10] V. A. J. Pyykkönen, S. Peotta, and P. Törmä, Suppression of nonequilibrium quasiparticle transport in flat-band superconductors, Phys. Rev. Lett. **130**, 216003 (2023).

[11] P. Törmä, S. Peotta, and B. A. Bernevig, Superconductivity, superfluidity and quantum geometry in twisted multilayer systems, Nat. Rev. Phys. **4**, 528 (2022).

[12] V. I. Iglovikov, F. Hébert, B. Grémaud, G. G. Batrouni, and R. T. Scalettar, Superconducting transitions in flat-band systems, Phys. Rev. B **90**, 094506 (2014).

[13] C. Poli, H. Schomerus, M. Bellec, U. Kuhl, and F. Mortessagne, Partial chiral symmetry-breaking as a route to spectrally isolated topological defect states in two-dimensional artificial materials, 2D Mater. **4**, 025008 (2017).

[14] T. T. Heikkilä and G. E. Volovik, Flat bands as a route to high-temperature superconductivity in graphite, in *Basic Physics of Functionalized Graphite*, edited by P. D. Esquinazi, Springer Series in Materials Science Vol. 244 (Springer International, Cham, 2016), pp. 123–143.

[15] T. T. Heikkilä, N. B. Kopnin, and G. E. Volovik, Flat bands in topological media, JETP Lett. **94**, 233 (2011).

[16] R. Mondaini, G. G. Batrouni, and B. Grémaud, Pairing and superconductivity in the flat band: Creutz lattice, Phys. Rev. B **98**, 155142 (2018).

[17] N. B. Kopnin, T. T. Heikkilä, and G. E. Volovik, High-temperature surface superconductivity in topological flat-band systems, Phys. Rev. B **83**, 220503(R) (2011).

[18] S. D. Huber and E. Altman, Bose condensation in flat bands, Phys. Rev. B **82**, 184502 (2010).

[19] B. Grémaud and G. G. Batrouni, Haldane phase on the sawtooth lattice: Edge states, entanglement spectrum, and the flat band, Phys. Rev. B **95**, 165131 (2017).

[20] N. Verma, T. Hazra, and M. Randeria, Optical spectral weight, phase stiffness, and $T_c$ bounds for trivial and topological flat band superconductors, Proc. Natl. Acad. Sci. **118**, e2106744118 (2021).

[21] W. Maimaiti, S. Flach, and A. Andreanov, Universal $d = 1$ flat band generator from compact localized states, Phys. Rev. B **99**, 125129 (2019).

[22] W. Maimaiti, A. Andreanov, and S. Flach, Flat-band generator in two dimensions, Phys. Rev. B **103**, 165116 (2021).

[23] D. Călugăru, A. Chew, L. Elcoro, Y. Xu, N. Regnault, Z.-D. Song, and B. A. Bernevig, General construction and topological classification of crystalline flat bands, Nat. Phys. **18**, 185 (2022).

[24] H. Kim, C. G. Oh, and J.-W. Rhim, General construction scheme for geometrically nontrivial flat band models, arXiv:2305.00448.

[25] Y. Hwang, J.-W. Rhim, and B.-J. Yang, General construction of flat bands with and without band crossings based on wave function singularity, Phys. Rev. B **104**, 085144 (2021).

[26] D. Leykam, A. Andreanov, and S. Flach, Artificial flat band systems: From lattice models to experiments, Adv. Phys.: X **3**, 1473052 (2018).

[27] M. N. Huda, S. Kezilebieke, and P. Liljeroth, Designer flat bands in quasi-one-dimensional atomic lattices, Phys. Rev. Res. **2**, 043426 (2020).

[28] J. Vidal, R. Mosseri, and B. Douçot, Aharonov-Bohm cages in two-dimensional structures, Phys. Rev. Lett. **81**, 5888 (1998).

[29] C. C. Abilio, P. Butaud, T. Fournier, B. Pannetier, J. Vidal, S. Tedesco, and B. Dalzotto, Magnetic field induced localization in a two-dimensional superconducting wire network, Phys. Rev. Lett. **83**, 5102 (1999).

[30] G.-B. Jo, J. Guzman, C. K. Thomas, P. Hosur, A. Vishwanath, and D. M. Stamper-Kurn, Ultracold atoms in a tunable optical kagome lattice, Phys. Rev. Lett. **108**, 045305 (2012).

[31] M. Hyrkäs, V. Apaja, and M. Manninen, Many-particle dynamics of bosons and fermions in quasi-one-dimensional flat-band lattices, Phys. Rev. A **87**, 023614 (2013).

[32] R. A. Vicencio, C. Cantillano, L. Morales-Inostroza, B. Real, C. Mejía-Cortés, S. Weimann, A. Szameit, and M. I. Molina, Observation of localized states in Lieb photonic lattices, Phys. Rev. Lett. **114**, 245503 (2015).

[33] T. T. Heikkilä and G. E. Volovik, Dimensional crossover in topological matter: Evolution of the multiple dirac point in the layered system to the flat band on the surface, JETP Lett. **93**, 59 (2011).

[34] N. B. Kopnin, M. Ijäs, A. Harju, and T. T. Heikkilä, High-temperature surface superconductivity in rhombohedral graphite, Phys. Rev. B **87**, 140503(R) (2013).

[35] T. Löthman and A. M. Black-Schaffer, Universal phase diagrams with superconducting domes for electronic flat bands, Phys. Rev. B **96**, 064505 (2017).

[36] E. Tang and L. Fu, Strain-induced partially flat band, helical snake states and interface superconductivity in topological crystalline insulators, Nat. Phys. **10**, 964 (2014).

[37] V. J. Kauppila, F. Aikebaier, and T. T. Heikkilä, Flat-band superconductivity in strained dirac materials, Phys. Rev. B **93**, 214505 (2016).

[38] A. Mallick, N. Chang, W. Maimaiti, S. Flach, and A. Andreanov, Wannier-Stark flatbands in Bravais lattices, Phys. Rev. Res. **3**, 013174 (2021).

[39] B. Anderson and M. Kasevich, Macroscopic quantum interference from atomic tunnel arrays, Science **282**, 1686 (1998).

[40] V. V. Ivanov, A. Alberti, M. Schioppo, G. Ferrari, M. Artoni, M. L. Chiofalo, and G. M. Tino, Coherent delocalization of atomic wave packets in driven lattice potentials, Phys. Rev. Lett. **100**, 043602 (2008).

[41] G. Roati, E. de Mirandes, F. Ferlaino, H. Ott, G. Modugno, and M. Inguscio, Atom interferometry with trapped Fermi gases, Phys. Rev. Lett. **92**, 230402 (2004).

[42] R. Sapienza, P. Costantino, D. Wiersma, M. Ghulinyan, C. J. Oton, and L. Pavesi, Optical analogue of electronic bloch oscillations, Phys. Rev. Lett. **91**, 263902 (2003).

[43] C. A. Hayward, D. Poilblanc, R. M. Noack, D. J. Scalapino, and W. Hanke, Evidence for a superfluid density in $t$-$J$ ladders, Phys. Rev. Lett. **75**, 926 (1995).

[44] W. Kohn, Theory of the insulating state, Phys. Rev. **133**, A171 (1964).

[45] D. J. Scalapino, S. R. White, and S. Zhang, Insulator, metal, or superconductor: The criteria, Phys. Rev. B **47**, 7995 (1993).

[46] T. Giamarchi, *Quantum Physics in One Dimension*, International Series of Monographs on Physics Vol. 121 (Clarendon Press, Oxford, 2003).

[47] The correlation function along the diagonal on the $z = 0$ band is 0 because of the global and local (within the flat band) half filling. This is due to the Fermi surface of the square lattice at half filling and does not mean that the particles are uncorrelated.

[48] M. Tovmasyan, S. Peotta, L. Liang, P. Törmä, and S. D. Huber, Preformed pairs in flat Bloch bands, Phys. Rev. B **98**, 134513 (2018).

[49] M. Thumin and G. Bouzerar, Flat-band superconductivity in a system with a tunable quantum metric: The stub lattice, Phys. Rev. B **107**, 214508 (2023).

[50] V. Emery, Theory of the quasi-one-dimensional electron gas with strong "on-site" interactions, Phys. Rev. B **14**, 2989 (1976).

[51] A. Mallick, N. Chang, A. Andreanov, and S. Flach, Anti-$\mathcal{PT}$ flatbands, Phys. Rev. A **105**, L021305 (2022).

[52] A. R. Kolovsky, A. Ramachandran, and S. Flach, Topological flat Wannier-Stark bands, Phys. Rev. B **97**, 045120 (2018).

[53] A. L. Kuzemsky, Variational principle of Bogoliubov and generalized mean fields in many-particle interacting systems, Int. J. Mod. Phys. B **29**, 1530010 (2015).